AD-A151 251

Entered)

PAGE

READ INSTRUCTIONS BEFORE COMPLETING FORM

1. REPORT NUMBER

2. GOVT ACCESSION NO.

3. RECIPIENT'S CATALOG NUMBER

4. TITLE (and Subtitle)

Application of Solidification Theory to Rapid Solidification Processing

5. TYPE OF REPORT & PERIOD COVERED
Semi-annual technical report
April 1, 1984 to Sept. 30, 1984

6. PERFORMING ORG. REPORT NUMBER

7. AUTHOR(s)

W. J. Boettinger, J. W. Cahn, S. R. Coriell
J. R. Manning and R. J. Schaefer

8. CONTRACT OR GRANT NUMBER(s)

ARPA Order 3751

9. PERFORMING ORGANIZATION NAME AND ADDRESS

Metallurgy Division
National Bureau of Standards
Gaithersburg, MD 20899

10. PROGRAM ELEMENT, PROJECT, TASK AREA & WORK UNIT NUMBERS

4D10
61101E

11. CONTROLLING OFFICE NAME AND ADDRESS

Materials Science Division
Defense Advanced Research Projects Agency
1400 Wilson Boulevard
Arlington, VA 22209

12. REPORT DATE
February 1985

13. NUMBER OF PAGES
12

14. MONITORING AGENCY NAME & ADDRESS(if different from Controlling Office)

15. SECURITY CLASS. (of this report)

15a. DECLASSIFICATION/DOWNGRADING SCHEDULE

16. DISTRIBUTION STATEMENT (of this Report)

Approved for public release. Distribution unlimited.

17. DISTRIBUTION STATEMENT (of the abstract entered in Block 20, if different from Report)

DTIC
ELECTE
MAR 14 1985
S D
E

18. SUPPLEMENTARY NOTES

19. KEY WORDS (Continue on reverse side if necessary and identify by block number)

Ag-Cu alloys; Alloy microstructures; Alloy microsegregation; Extended solid solubility; NiAl-Cr alloys; Quasi-binary alloys; Rapid solidification; Solidification theory

(nickel aluminum—chromium silver-15)

20. ABSTRACT (Continue on reverse side if necessary and identify by block number)

Solidification theory can be used to predict and control processes occurring during rapid solidification. Two papers prepared for publication provide results showing such predictions. (1) The effects of rapid solidification velocity on microstructure and phase solubility extension in ~~NiAl-Cr~~ quasibinary alloys are reported. (2) Segregation behavior and microstructural spacings in ~~Ag-15~~ wt% Cu alloys are reported as a function of solidification velocity around and below the transition velocity from cellular to banded microstructures.

copper

DTIC FILE COPY

DD FORM 1 JAN 73 1473 EDITION OF 1 NOV 65 IS OBSOLETE

85 03 01 006

SECURITY CLASSIFICATION OF THIS PAGE (When Data Entered)

Application of Solidification Theory to Rapid Solidification Processing

W. J. Boettinger, J. W. Cahn, S. R. Coriell,
J. R. Manning, and R. J. Schaefer
Metallurgy Division
Center for Materials Science
National Bureau of Standards
Gaithersburg, MD 20899

Semi-Annual Technical Report
Period Covered: April 1, 1984 to September 30, 1984

Report Issued: February 1985

Prepared for
Defense Advanced Research Projects Agency
Arlington, VA 22209

Program Code No: 4D10
Effective Date of Contract: April 1, 1979
Contract Expiration Date: September 30, 1986
Principal Investigator: J. R. Manning (301/921-3354)

Table of Contents

Application of Solidification Theory to Rapid Solidification Processing

This semi-annual technical report for ARPA Order 3751 covers the period April 1, 1984 to September 30, 1984.

Task Objective

The objective of this work is to develop guidelines based on the kinetic and thermodynamic aspects of solidification theory for prediction and control of rapid solidification processes. In particular, segregation effects and rules governing the formation of equilibrium and non-equilibrium phases, including metallic glasses, will be investigated. Areas where microstructural opportunities exist for significant improvements in alloy properties will be emphasized.

Technical Problem and General Methodology

Rapid solidification techniques make it possible to produce new types of materials having significantly better properties than conventionally processed materials. However, improved predictive techniques and control of rapid solidification processes are needed. The current studies are focussed on the science underlying areas where improved materials can be obtained in order to provide such prediction and control. This work is both theoretical and experimental.

Two major ways in which rapid solidification technology provides improved materials are:

1. Production of alloys with new compositions and phases.
2. Production of improved alloy properties by control of microstructures and homogeneity in rapidly solidified alloys.

The general method followed in this work has been to identify critical questions in these major rapid solidification application areas where solidification theory, when properly developed and checked by experiment, can provide improved understanding of important rapid solidification processes. This understanding then is pursued to provide guidelines that can be used by alloy producers to obtain new improved materials and to select optimum alloy compositions and processing conditions for rapid solidification applications.

Technical Results

1. Production of Alloys with New Compositions or Phases -- Extended Solid Solubility

Rapid solidification, if it is sufficiently rapid, can prevent the separation of alloy constituents into equilibrium phases during solidification and allow the freezing-in of metastable phases, for example, metallic glass phases or other phases not normally found by conventional solidification. These new phases can have properties that are drastically different from the properties of the equilibrium phases. The conditions for producing such rapidly solidified alloys having compositions in two-phase regions of alloy phase diagrams are being investigated. It has been found that in some cases, such as Ag-Cu, homogeneous crystalline alloys can be produced by partitionless solidification if the solidification velocity is above a critical value, dependent on composition. In other more complex cases, such as NiAl-Cr a different crystal structure than might have been expected can be produced by rapid solidification in the two-phase region. In other cases, entirely new phases can be produced. Work in this project is continuing on new phases found in Al-Mn (and other rapidly solidified alloys) and on precipitation

processes in rapidly solidified Al-Cr alloys. It is believed that the new phases and structures being produced in these alloys may have great scientific and practical importance.

One of the major ways in which rapid solidification can be expected to lead to technological and scientific breakthroughs is by producing entirely new types of alloys that cannot be produced by conventional means. For this reason, one of the main emphases of the present work has been to investigate phenomena in the extended solid solubility regime. This composition regime is not normally accessible for investigation by conventional metallurgy and hence is a regime where new and unexpected effects and processes are more likely to be found.

In work completed during the reporting period, a paper was written on "The Effect of Rapid Solidification Velocity on Microstructure and Phase Solubility Extension in NiAl-Cr Quasibinary Eutectic" by W. J. Boettinger, D. Shechtman, T. Z. Kattamis and R. J. Schaefer. A copy of this paper is included as part of this report in the Appendix. This work was done in collaboration with D. Shechtman, Johns Hopkins University and the Technion, and T. Z. Kattamis, University of Connecticut, during times they spent at the National Bureau of Standards

2. Production of Improved Alloy Properties by Control of Microstructures and Homogeneity in Rapidly Solidified Alloys

Even in cases where the equilibrium solid solubility is not exceeded, it is frequently possible to obtain striking improvements in alloy properties by means of rapid solidification. These improvements result from the differences in alloy microstructure and homogeneity produced by rapid solidification.

Previous work in silver-rich Ag-Cu done on this project has mapped out regions in a plot of composition vs. electron beam scan velocity (closely related to solidification velocity) where particular types of microstructures could be found. At the highest solidification velocities, microsegregation-free alloys were produced, either by creation of planar solidification interfaces or by partitionless solidification. By contrast, at the lower solidification velocities (below a scan velocity of approximately 20 cm/s, the exact value depending on composition), cellular microstructures formed with segregation of Cu to the intercellular regions.

At intermediate velocities for compositions above the equilibrium solubility limit (approximately 9 wt% Cu), a banded microstructure was found, alternating between microsegregation-free bands and cellular structured bands normal to the solidification direction. Since variations in the spacings and other features in the cellular regime can vary significantly with solidification velocity, alloys with solidification velocities around and below the transition velocity from cellular microstructure to banded were examined for Ag-15 wt% Cu alloys. Changes in segregation behavior and microstructural spacings were determined. Some results from this work were reported in a paper "Cellular Microsegregation in Rapidly Solidified Ag-15 wt% Cu Alloy" by L. A. Bendersky and W. J. Boettinger. A copy of this paper is included as part of this report in the Appendix. This work was done in collaboration with L. A. Bendersky, Johns Hopkins University, during time he spent at the National Bureau of Standards.

"Fifth International Conference on Rapidly Quenched Metals," Wurzburg FRG, September 3-7, 1984.

THE EFFECT OF RAPID SOLIDIFICATION VELOCITY ON MICROSTRUCTURE AND PHASE SOLUBILITY EXTENSION IN NiAl-Cr QUASIBINARY EUTECTIC

W. J. BOETTINGER

Metallurgy Division, National Bureau of Standards, Washington, D.C., USA

D. SHECHTMAN*

Technion, Haifa, Israel and Center for Materials Research, Johns Hopkins University, Baltimore, MD, USA

T. Z. KATTAMIS*

University of Connecticut, Storrs, CT, USA

R. J. SCHAEFER

Metallurgy Division, National Bureau of Standards, Washington, D.C., USA

The transition from a two-phase rod-type eutectic microstructure to a single-phase Cr-supersaturated NiAl microstructure for the NiAl-Cr quasibinary eutectic composition is determined as a function of growth rate by electron beam melting and solidification scans. At growth rates below 1 cm/s the alloy exhibits a two-phase eutectic structure. Above 2.5 cm/s the structure solidifies as single phase Cr-supersaturated NiAl which subsequently decomposes spinodally.

1. INTRODUCTION

The NiAl-Cr quasibinary eutectic composition is Ni-33 at% Al-34 at% Cr and is of interest for the study of extended solubility because of the similarity of crystal structures (CsCl for β-NiAl and BCC for α-Cr) and lattice parameters of the two phases in the eutectic.[1] Previous work[2] has shown that melt spun ribbons exhibit a variety of microstructures: extremely fine eutectic, supersaturated β-NiAl phase (which undergoes solid state decomposition) and a mixture of the two. The thermodynamic possibility of solubility extension of the two phases was evaluated using T_0 curves and was found to be consistent with the formation of supersaturated β-NiAl rather than α-Cr from eutectic melts.

The present work seeks to establish the kinetic aspects of the transition from eutectic growth at low solidification rates to the supersaturated single phase structure observed in melt spun ribbons. By careful microstructural analysis of the shape of molten pools during electron beam surface scans performed at speeds between 0.1 cm/s and 50 cm/s, the local growth rate within solidified zones is determined and correlated to the local microstructure obtained by TEM.

2. EXPERIMENTAL PROCEDURE

Rapidly solidified samples were prepared using one dimensional scans of a focussed electron beam across the surface of the alloy.[3] These scans produce a melted and resolidified trail, typically 0.5 mm wide and 0.1 mm deep. Due to the relatively poor thermal diffusivity of the alloy, the growth direction, even at the top center of the trail, differs significantly from the scan direction. Under steady state

* Guest Workers, Metallurgy Division, National Bureau of Standards, Washington, D.C., USA

conditions, the true growth rate, V, is the product of the scan velocity with the cosine of the angle between the growth direction and the scan direction. For scan speeds below 2.5 cm/s these angles were measured for each specimen by longitudinal sections through the trail centerline and were typically 30°. The measured angles were employed to describe the growth rate for the microstructures. For scan speeds above 2.5 cm/s the angles were not measured but are estimated to be about 60° leading to a 50% reduction of the actual growth rate compared to the scan rate. TEM specimens were prepared by ion milling full disks cut parallel to the surface of the alloy or half disks cut perpendicular to the scan direction. In all cases care was taken to locate the thin area near the top center of the melted trail where the growth rate is known from the above arguments.

3. RESULTS

For growth rates below 1 cm/s the alloy solidifies as a fine eutectic structure of β-NiAl and α-Cr phases as shown in Fig. 1. The observed eutectic spacings, λ_e, are plotted on the left side of Fig. 4 along with an extrapolation of the relationship between spacing and growth rate determined at slower rates by

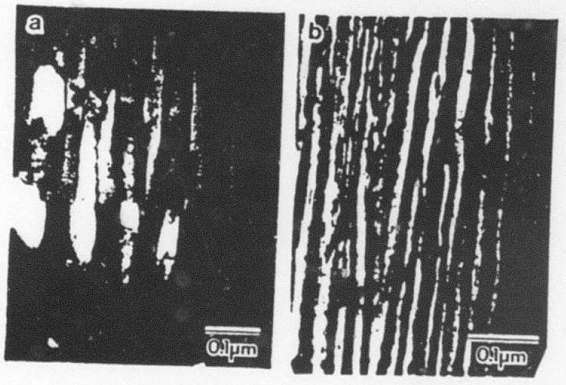

Fig. 1. Eutectic structures of α-Cr and β-NiAl solidified at (a) 0.09 cm/s and (b) 0.8 cm/s with spacings of ~ 80 nm and ~ 20 nm respectively. TEM.

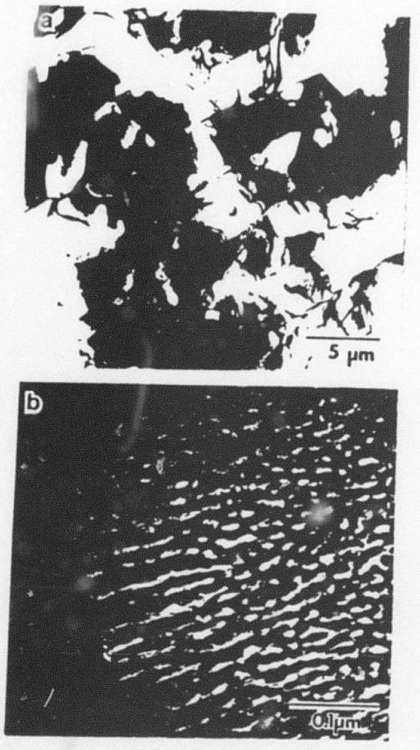

Fig. 2. (a) Columnar grains of supersaturated β-NiAl produced at 2.5 cm/s (oblique section).
(b) Fine structure of decomposed supersaturated β-NiAl. TEM.

Walter and Cline.[4] ($\lambda_e^2 V = 7 \times 10^{-12}$ cm^3/s) For eutectic growth at rates on the order of 1-10 cm/s, the interfacial undercooling due to solute redistribution and interface curvature becomes sufficiently large that the temperature dependence of the liquid diffusion becomes important.[3] Hence the $\lambda_e^2 V$ relationship cannot be extrapolated past this range. In fact, in the present case at a growth rate of 2.5 cm/s and above, the alloy does not solidify as with a eutectic structure.

Fig. 2 shows the microstructure obtained at 2.5 cm/s. It consists of columnar grains of β-NiAl which have undergone spinodal decomposition. The average composition appears quite uniform across the grain interiors as

judged by the uniformity of the decomposition structure across the grains. Antiphase domains (not shown) are present within the grains with sizes which are very large compared to the scale of the spinodal structure. This fact indicates that the structure was ordered before it decomposed and consequently that the supersaturated β-NiAl formed directly from the melt. Identical structures were obtained in melt-spun ribbons[2].

A high magnification view of the nature of the region near a grain boundary is shown in Fig. 2b. On the right is seen the spinodal structure present throughout the grains. The structure shows no direction of elongation regardless of the plane of section and therefore is not eutectic. On the left, close to the edge of the grain, a fine structure aligned perpendicular to the boundary is present. Even though this resembles a fine eutectic, it is thought to arise in the solid state by a peculiarity of coarsening of the spinodal structure near a grain boundary.[5] In melt spun ribbons,[2] similar structures were observed but also intergranular regions which were clearly composed of eutectic. This latter structure was not seen in the electron beam melted specimens, possibly due to the absence of recalescence effects in surface melted specimens.

The general features of the microstructure do not vary significantly at increased growth rates (see Fig. 3) except that the spinodal spacing decreases with increasing growth rate. These spacings are shown on the right side of Fig. 4.

4. DISCUSSION

Three topics warrant discussion in the present paper: (1) the existence of a maximum growth rate of ~ 1-2 cm/s for the α-Cr and β-NiAl eutectic; (2) the formation of the supersaturated β-NiAl phase at the relatively low growth rates of 2.5 cm/s and above; and

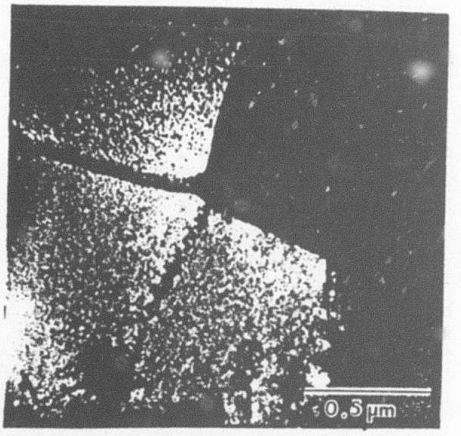

Fig. 3. Transverse section of columnar grains of supersatured β-NiAl produced at 50 cm/s showing pairs of dislocations in the ordered structure at a low angle grain boundary. TEM.

(3) the refinement of the spinodal spacing with increasing growth rate.

4.1 Eutectic Growth Rate Maximum

The observed growth rate maximum for the eutectic structure is consistent with theoretical arguments and results on other systems.[3] Inclusion of the temperature dependence of the liquid diffusion coefficient into eutectic growth theory predicts a maximum growth rate in the range of 1-10 cm/s for most eutectics. This modification of the theory also leads to a modification of the $\lambda_e^2 V$ relationship obtained at slow rate. However this modification only becomes detectable experimentally very close to the growth rate maximum. This fact is reflected in the present work by the good agreement of the measured eutectic spacings with the extrapolated $\lambda_e^2 V$ relation of Cline and Walter. Presumably measurements of spacings between 1 and 2.5 cm/s would show a marked deviation from the extrapolated $\lambda_e^2 V$ relationship.

4.2 Supersaturated β-NiAl

As described previously,[2] the formation of β-NiAl by partitionless solidification from

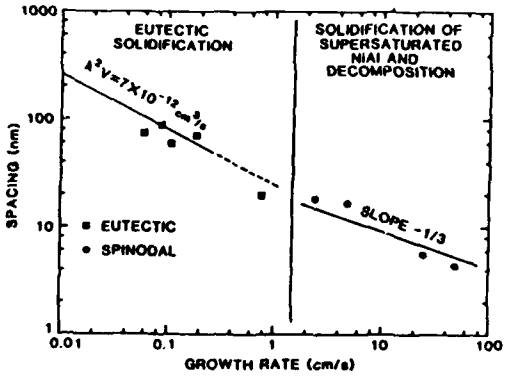

Fig. 4. Eutectic spacing observed at low velocity and spinodal spacing in decomposed supersaturated β-NiAl observed at high velocity as a function of growth rate.

liquid of eutectic composition is thermodynamically favored over the formation of α-Cr. This conclusion is based on an analysis of the T_0 curves of the NiAl-Cr quasibinary system. Partitionless solidification not only requires interface undercooling below the T_0 curve but also growth at sufficiently high rates to cause solute trapping. For dilute alloys, this rate is thought to be near or less than the ratio of the liquid diffusion coefficient to the interatomic dimensions or about 5 m/s for most metallic systems. Therefore, the formation of the supersaturated β-NiAl structure at growth rates as low as 2.5 cm/s in the present work is quite surprising. One possible reason for this result lies in the fact that the velocity required for partitionless solidification in concentrated alloys may be smaller than that required for dilute alloys.[6-7] Such a trend is seen in Ag-Cu alloys where a growth rate of 7 m/s (compared to 5 m/s) was required for alloys of eutectic composition.[3] Another explanation for this result could lie in the fact that partitionless solidification has not occurred. Planar growth with equilibrium partitioning with solid forming at the metastably extended solidus curve can produce microsegregation-free solids.[6] The published phase diagram data[8] is sparse but would be inconsistent with this second possibility. Future analysis of this result is necessary.

4.3 Spinodal Spacing

For the case of a moving heat source the average cooling rate in the solid behind the freezing interface can be estimated as being proportional to the source speed, V. For the case of continuous cooling the spinodal spacing, λ_S, should vary as a power of the solid cooling rate.[9] For the present case where extensive coarsening has taken place the power is roughly -1/3[5] and hence $\lambda_S \sim V^{-1/3}$. The variation of spinodal spacing with electron beam scan rate in Fig. 4 is not inconsistent with this relationship.

REFERENCES

1. J. L. Walter, H. E. Cline and E. F. Koch, Trans. TMS-AIME 245 (1969) 2073.
2. D. Shechtman, W. J. Boettinger, T. Z. Kattamis, and F. S. Biancaniello, Acta Met. 32 (1984) 749.
3. W. J. Boettinger, D. Shechtman, R. J. Schaefer and F. S. Binacaniello, Met. Trans 15A (1984) 55.
4. J. L. Walter and H. E. Cline, Metall. Trans. 1, (1970) 1221.
5. J. W. Cahn, private communication.
6. W. J. Boettinger, S. R. Coriell and R. F. Sekerka, Mat. Sci. & Eng. (1984).
7. M. J. Aziz, Appl. Phys. Lett 43 (1983) 552.
8. I. I. Kornilov and R. C. Mintz, Kokl. Akad. Nauk. USSR 94, (1954) 1085.
9. E. I. Huston, J. W. Cahn and J. E. Hilliard, Acta Met. 14 (1966) 1053.

"Fifth International Conference on Rapidly Quenched Metals," Wurzburg FRG, September 3-7, 1984

ELLULAR MICROSEGREGATION IN RAPIDLY SOLIDIFIED Ag-15 wt% Cu ALLOYS

. A. BENDERSKY*

enter for Materials Research, The Johns Hopkins University, Baltimore, MD, USA

. J. BOETTINGER

etallurgy Division, National Bureau of Standards, Washington, DC, USA

Microstructural and microchemical analysis has been performed on Ag-15 wt% Cu alloys produced y electron beam melting with solidification velocities of 2.5, 12 and 18 cm/s. Cellular structures f the Ag-rich phase are produced with spacings of 0.8, 0.3 and 0.2μm, respectively. Intercellular egions contained fine eutectic at the lowest speed but only Cu-rich phase at the higher speeds. ie composition within the cells was found to be nearly uniform and 12.5 ± 1 wt% Cu. The uniformity id level of the Cu content within the cells are discussed.

. INTRODUCTION

Many rapidly solidified crystalline alloys khibit very fine cellular microsegregation ıtterns. The amount of solute incorporated ıto the cell interiors has a strong influence ı the volume fraction of intercellular phases id precipitation in the cell interiors during ıbsequent thermomechanical treatment. At ıtremely high rates of solidification (~1 m/s), crosegregation-free alloys may be produced ' solute trapping.[1] However, many important ıpid solidification processes do not impose ch high growth rates. Hence the details of crosegregation patterns were examined at wer growth rates where significant solute apping is not expected.

Several authors have measured cellular lute profiles in rapidly solidified alloys oduced with unknown or calculated growth tes.[2-5] In the present work the growth te is determined experimentally using the ctron beam melting and resolidification :hnique.[6]

The theory of alloy dendritic and/or lular growth under conditions of local interfacial equilibrium is being continually refined.[7-8] Solari and Biloni,[9] using the model of Burden and Hunt[10] for the tip concentration, have modeled the entire microsegregation profile as a function of growth rate under the assumption of no lateral concentration gradients in the liquid between solidifying cells. Such an approach is only valid when the cell spacing, λ_1, is much less than D/V, where D is the liquid diffusion coefficient and V is the growth rate. As will be shown in the present paper, this assumption is questionable for rapid solidification.

2. EXPERIMENTAL PROCEDURE

Rapidly solidified samples were prepared using one dimensional scans of a focussed electron beam across the surface of a Ag-15 wt% Cu sample at speeds of 2.5, 12, and 18 cm/s. Due to the relatively high thermal diffusivity of Ag, the growth direction and solidification speed of the resolidified alloy near the top center of the melted region is nearly parallel and equal to the electron beam scan velocity. TEM samples were prepared by ion milling on a

---

est worker, Metallurgy Division, National Bureau of Standards, Washington, DC, USA.

liquid nitrogen cooled stage thin half disks cut transverse to the scan direction.

Composition profiles were determined using analytical electron microscopy. Compositions were quantified using the Cliff-Lorimer ratio technique[11] for the L_α and K_α x-rays for Ag and Cu with a constant determined experimentally from measurements on a homogeneous Ag-28 wt% Cu alloy, rapidly solidified in a partitionless manner at a velocity of 70 cm/sec.[6] The thin-film criterion[11] is satisfied for a specimen thickness less than 153 nm for both characteristic x-rays. The usual thickness of specimens was less than 150 nm. The spatial resolution was determined using the beam broadening equation.[11] For the foil thickness, 150 nm, the beam broadening was calculated to be 42 nm, and the total broadening with the probe size 5 nm (in our experiments) was 42.2 nm.

3. RESULTS AND DISCUSSION

3.1 Microstructure

Figure 1 shows micrographs of cellular structures of Ag-rich phase seen in Ag-15 wt% Cu alloys solidified at 2.5, 12, and 18 cm/s. The distance between cells are approximately 0.8, 0.3, and 0.2 μm respectively. Note that these values when divided by D/V, the characteristic diffusion length, are in excess of 10. (D is taken as 2×10^{-5} cm^2/s).

The volume fraction of intercellular regions is small compared to that found in conventionally cast alloy of the same composition. This is due to the high level of solute present in the cell interiors (see Section 3.2). At a growth rate of 2.5 cm/s (Fig. 1a), those intercellular regions which are wide, contain a fine eutectic structure of the Ag- and Cu-rich phases. The eutectic spacing is ~48 nm. In narrow intercellular regions, only the Cu-rich phase is seen. This feature, which also occurs in ordinary cast microstructures, is called a divorced eutectic and is present whenever the

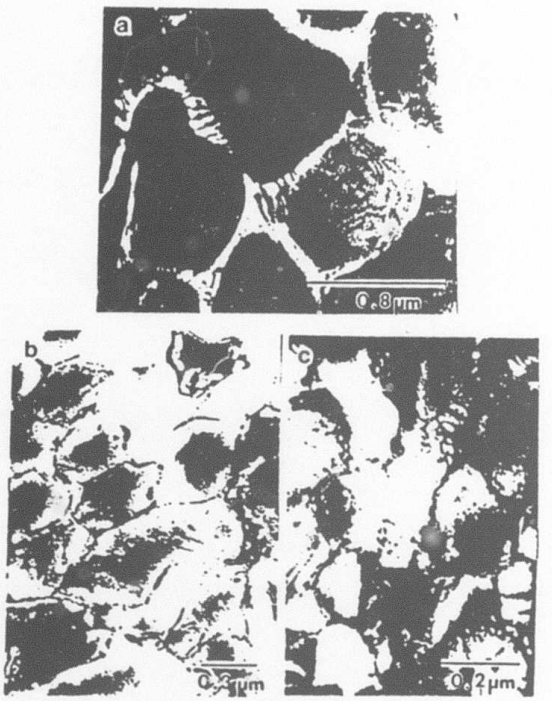

Fig. 1. Cellular structures in Ag-15 wt% Cu solidified at (a) 2.5 cm/s (dark field), (b) 12 cm/s, and (c) 18 cm/s. TEM.

width of an intercellular region is smaller than the eutectic spacing which would occur at the imposed growth rate.

Figure 2 shows a high magnification micrograph of intercellular regions typical of those seen at 12 and 18 cm/s. No eutectic is seen at these growth rates. The intercellular regions

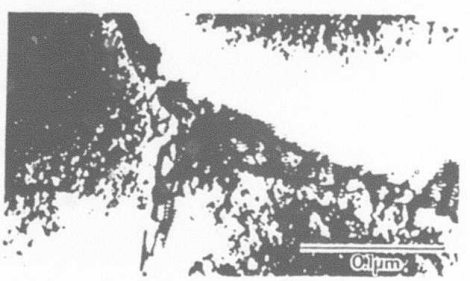

Fig. 2. Intercellular region in alloy solidified at 12 cm/s. TEM.

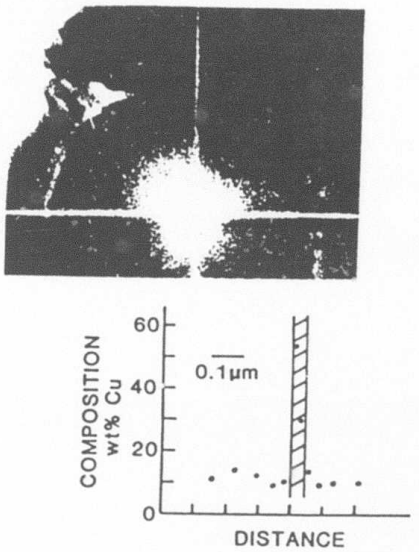

Fig. 3. STEM micrograph and composition profile across intercellular region of alloy solidified at 2.5 cm/s.

are comprised solely of the Cu-rich phase (fringe pattern). This divorced eutectic occurs for a different reason at high growth rates. It is known that the Ag-Cu eutectic cannot grow faster than 2.5 cm/s.[6] Hence the eutectic should also be absent as an intercellular microconstituent at growth rates higher than 2.5 cm/s.

3.2. Microanalysis

Figure 3 shows a STEM micrograph and an associated microanalysis profile of the relatively coarse cellular structure formed at 2.5 cm/s. Typical spatial and composition resolutions are 40 nm and 2 wt% Cu. Within these limitations, the composition of the cell interiors is uniform with 11.8 ± 1.3 wt% Cu. The measured compositions in the cell walls are lower than the true composition due to the beam broadening and the fact that the cell wall is slightly oblique to the electron beam with Ag-rich phase also being probed. In regions of the foil where the Ag-rich phase has been completely removed by ion milling, the composition of the Cu-rich intercellular phase was found to be ~90 wt% Cu.

A similar profile for finer cells grown at 12 cm/s is shown in Figure 4. The cell interior is uniform with 12.3 ± 1.2 wt% Cu. The center composition of a number of the very fine cells produced at 18 cm/s were measured as shown in Figure 5. The average of these measurements was 13.6 ± 1.6 wt% Cu.

Two aspects of these profiles warrant discussion: the uniformity of the compositions within the cells and the level of solute within the cells. The slight increase in cell compositions from 11.8 to 13.6 wt% Cu with increasing

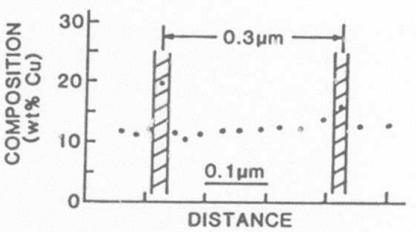

Fig. 4. Composition profile across a cell solidified at 12 cm/s.

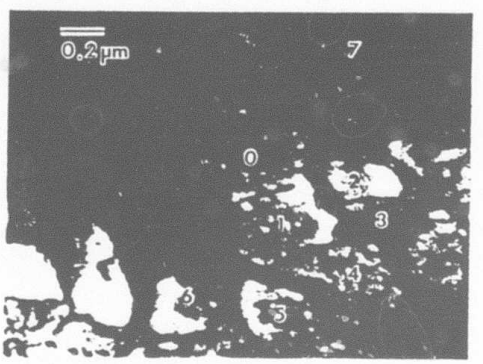

Fig. 5. STEM micrograph of cellular structure solidified at 18 cm/s. The compositions at the centers of the cells marked 0, 1, . . . 7 respectively are 12.5, 13.0, 13.8, 15.5, 14.8, 13.8, 12.0, 13.2 wt% Cu.

growth rate cannot be documented with certainty in the present work and the solute level of all the cells will be taken as ~12.5 wt% Cu.

At growth rates used in the present work, the assumption of local interfacial equilibrium at the liquid/solid interface should be valid[1] and in fact partitionless solidification is only observed in Ag-15% Cu at growth rates above 2 m/s.[7] Hence the phase diagram is of interest. Recently Murray[12] included in her assessment an evaluation of the free energy of the phases which permits the calculation of the metastable Ag-rich solidus below the eutectic temperature. The solidus has a metastable retrograde at 10.5 wt% Cu and 700°C. Under interfacial equilibrium conditions solid cannot form with composition higher than the retrograde composition. The observed level of solute in the cells is very close to the retrograde composition. The agreement may be even better considering the fact that minor adjustments of the free energy functions can increase this retrograde composition by a few percent.[13]

The observation of uniform compositions across cell interiors but with a high degree of segregation to the cell walls is a seemingly curious result. Mazur and Flemings[2] in work on Al-Cu did not see uniformity within cell interiors. However the spacings of the cells measured in their work were greater than 2 μm whereas the cells measured in the present work are less than 1 μm.

The theory of Solari and Biloni,[9] while predicting a reduced level of microsegregation at high growth rates, does not predict uniform profiles within cell interiors. This is due to their assumption which does not allow lateral solute gradients. Non-equilibrium trapping of solute is often used as an explanation of flat microsegregation profiles. However, McFadden and Coriell[14] have numerically calculated solute concentrations, temperature fields and interface shapes for two-dimensional cellular interfaces in a self-consistent manner. They have shown that compositions may be quite uniform across the major fraction of a cell with strong segregation to cell walls even when local equilibrium exists at the liquid-solid interface. Such microsegregation profiles should be very common whenever $10 < \frac{\lambda_1 V}{D} < 100$. Such is the case in the present experiments.

ACKNOWLEDGEMENT

The authors wish to thank S. R. Coriell, G. B. McFadden and R. J. Schaefer for many helpful discussions.

REFERENCES

1. W. J. Boettinger, S. R. Coriell, and R. F. Sekerka, Mat. Sci. & Eng., 65 (1984), 27.
2. L. J. Mazur and M. C. Flemings, Proc. 4th Int. Conf. on Rapidly Quenched Metals, Vol. 2, T. Mazumoto, Suzuki, eds., Japan Inst. of Metals, Sendai (1982), 1557.
3. T. Z. Kattamis and R. Mehrabian, J. Mat. Sci. 9 (1974) 1446.
4. T. F. Kelly, G. B. Olson, and J. B. Vander Sande, in Rapidly Solidified Amorphous and Crystalline Alloys, B. H. Kear, B. C. Giessen, and M. Cohen eds., North Holland, 1982, 343.
5. H. Palacio, M. Solari, and H. Biloni in Physical Metallurgy, Part 1 ed. by R. W. Cahn and P. Haasen, North Holland, Amsterdam (1983), 526.
6. W. J. Boettinger, D. Shechtman, R. J. Schaefer, F. S. Biancaniello, Met. Trans, 15A, 55, 1984.
7. R. Trivedi, J. Cryst. Growth 49, (1980), 219.
8. W. Kurz and D. J. Fisher, Acta Met. 29 (1981), 11.
9. M. Solari and H. Biloni, J. Cryst. Growth 49 (1980), 451.
10. M. H. Burden and J. D. Hunt, J. Cryst. Growth 22 (1974), 109.
11. J. I. Goldstein, Introduction to Analytical Electron Microscopy, eds. J. J. Hren, J. I. Goldstein, and D. C. Joy, Plenum Press, NY, 1979, p. 83.
12. J. F. Murray, Met. Trans, 15A (1984), 261.
13. J. F. Murray, private communication.
14. G. B. McFadden and S. R. Coriell, Physica D (1984), in press.